Friction Force Spectroscopy of β- and κ-Casein Monolayers

ARTICLE *in* LANGMUIR · FEBRUARY 2011

Impact Factor: 4.46 · DOI: 10.1021/la1043377 · Source: PubMed

3 AUTHORS, INCLUDING:

Javier Sotres
Malmö University
40 PUBLICATIONS **426** CITATIONS
SEE PROFILE

Olof Svensson
Lund University
12 PUBLICATIONS **204** CITATIONS
SEE PROFILE

Langmuir
Article
pubs.acs.org/Langmuir

Friction Force Spectroscopy of β- and κ-Casein Monolayers

Javier Sotres,* Olof Svensson, and Thomas Arnebrant

Biomedical Laboratory Science and Technology, Faculty of Health and Society, Malmoe University, 20506 Malmoe, Sweden

Received May 26, 2010. Revised Manuscript Received December 7, 2010

Friction force spectroscopy (FFS) has been applied to study the tribological properties of β- and κ-casein layers on hydrophobic substrates in aqueous solutions. Nanometer-sized imaging tips were employed. This allowed exerting and determining the high pressures needed to remove the layers and registering the topographic evolution during this process. Both β- and κ-casein layers showed similar and not particularly high initial frictional responses (friction coefficient of ∼1 when measured with a silicon nitride tip). The pressures needed to remove the layers were of the same order of magnitude for both proteins, $\sim 10^8$ Pa, but slightly higher for those composed of β-casein. The technique has also shown to be useful in studying the two-dimensional lateral diffusion of the proteins and the wear on the layers they form.

1. Introduction

Caseins, the most abundant milk proteins, are synthesized in the mammary gland and secreted as large calcium-dependent aggregates known as casein micelles.[1] A common characteristic of all caseins is the high amount of prolines in the peptide chain. These residues are known to prevent the formation of α-helices and β-sheets, resulting in the absence of an ordered tertiary structure and, thus, in the exposure of most of their residues to the surrounding medium.[2] This characteristic, along with their considerable electrostatic charge, the alternation between hydrophilic and hydrophobic domains, and their phosphorylation and glycosylation sites, confers these molecules with highly valued surface-active and colloid-stabilizing properties.[3]

Bovine milk has been studied to a much higher extent than milk from any other source. Four major bovine caseins (α_{s1}, α_{s2}, β, and κ) have been identified. These proteins can be classified with respect to different aspects. One is the distribution of their hydrophobic and hydrophilic domains. While in α_s-caseins these domains are alternating, β- and κ-casein have a marked amphiphilic nature with the subsequent tendency for self-association. Their amphiphilic character makes β- and κ-caseins good candidates to stabilize emulsions or suspensions. The emulsifying properties of β-casein, a molecule which can form micelles at concentrations above ∼0.5 $mg \cdot mL^{-1}$,[4] have been widely proved.[3,5] By contrast, the tendency of κ-casein to exist in the form of disulfide-linked oligomers[6] lowers its efficiency as an emulsifying agent, and little attention has been paid to study κ-casein layers on hydrophobic/hydrophilic interfaces.[7−9] Caseins can also be classified regarding their sensitivity to calcium:[10] α_s-caseins precipitate by very small amounts of calcium, β-casein by moderate amounts of calcium, while κ-casein is calcium insensitive. This is mainly a consequence of the post-translational modifications: α_s-caseins and β-casein are highly phosphorylated proteins, while in κ-casein a much lower degree of phosphorylation is combined with the presence of a variable number of carbohydrate moieties.[11] The post-translationally added moieties in both β- and κ-casein are located mainly in their hydrophilic regions. Thus, it is reasonable to assume that these modifications will have a strong impact on the interfacial properties of casein films.

The study of adsorbed casein films is not an easy issue. Standard methods for structural analysis, such as crystallography, NMR, and circular dichroism, either are impossible to apply or provide only limited information. This is because either the proteins are immobilized on an interface or the emulsions containing the proteins give rise to extremely high light scattering.[12] For this reason, more indirect methods have been usually applied in the study of these systems. The mass distribution in the adsorbed films could be monitored by small-angle X-ray scattering[13] and by neutron reflectance.[14] The hydrodynamic thickness of the layers could be inferred from dynamic light scattering experiments.[15] The study of these systems has also been approached by highly sensitive surface techniques such as ellipsometry,[7,8,16] surface plasmon resonance (SPR),[17] Brewster angle microscopy (BAM),[18] and quartz crystal microbalance (QCM).[19] An interesting approach has been the use of the surface force apparatus (SFA) to study the interactions between caseins layers.[20,21] The surface topography of

*To whom correspondence should be addressed. E-mail: javier.sotres@mah.se.

(1) Horne, D. S. *Curr. Opin. Colloid Interface Sci.* **2006**, *11*, 148–153.
(2) Swaisgood, H. E. *J. Dairy Sci.* **1993**, *76*, 3054–3061.
(3) Dickinson, E. *Colloids Surf., B* **2001**, *20*, 197–210.
(4) Schmidt, D. G.; Payens, T. A. J. *J. Colloid Interface Sci.* **1972**, *15*, 161–176.
(5) Ai, Y.; Wei, D. *J. Macromol. Sci.* **2007**, *45*, 456–461.
(6) Rasmussen, L. K.; Johsen, L. B.; Tsiora, A.; Sørensen, E. S.; Thomsen, J. K.; Nielsen, N. C.; Jakobse, H. J.; Petersen, T. E. *Int. Dairy J.* **1999**, *9*, 215–218.
(7) Arnebrant, T.; Nylander, T. *J. Colloid Interface Sci.* **1986**, *111*, 529–533.
(8) Vie, V.; Moreno, J.; Beaufils, S.; Lesniewska, E.; Leonil, J.; Renault, A. *Single Mol.* **2002**, *2*−*3*, 127–133.
(9) Gerung, A. M.D. Thesis, Texas A&M University, 2005.
(10) Fiat, A. N.; Jolles, P. *Mol. Cell. Biochem.* **1989**, *87*, 5–30.
(11) Swaisgood, H. E. In *Advanced Dairy Chemistry*, 3rd ed.; Fox, P. H., McSweeney, P. L. H., Eds.; Elsevier: London/New York, 2003; Vol. *1*, p 156.
(12) Dalgleish, D. G. *Food Res. Int.* **1996**, *29*, 541–547.
(13) Mackie, A. R.; Mingins, J.; North, A. N. *J. Chem. Soc., Faraday Trans.* **1991**, *87*, 3043–3049.
(14) Nylander, T.; Tiberg, F.; Su, T. J.; Lu, J. R.; Thomas, R. K. *Biomacromolecules* **2001**, *2*, 278–287.
(15) Dalgleish, D. G.; Leaver, J. *J. Colloid Interface Sci.* **1991**, *141*, 288–294.
(16) Kull, T.; Nylander, T.; Tiberg, F.; Wahlgren, N. M. *Langmuir* **1997**, *13*, 5141–5147.
(17) Marchesseau, S.; Mani, J. C.; Martineau, P.; Roquet, F.; Cuq, J. L.; Pugniere, M. *J. Dairy Sci.* **2002**, *85*, 2711–2721.
(18) Rodriguez Patino, J. M.; Sanchez, C. C.; Rodriguez Niño, M. R. *Food Hydrocolloids* **1999**, *13*, 401–408.
(19) Yan, Y.; Hu, J.; Yao, P. *Langmuir* **2009**, *25*, 397–402.
(20) Chowdhury, P. B.; Luckham, P. F. *Colloids Surf., B* **1995**, *4*, 327–334.
(21) Nylander, T.; Wahlgren, N. M. *Langmuir* **1997**, *13*, 6219–6225.

these layers has also been characterized by atomic force microscopy (AFM).[8,22] Moreover, the combination of many of these techniques with selective proteolysis of the proteins has provided valuable structural information of these layers both at oil/water interfaces[23] and at solid/liquid interfaces.[14,16] The mechanical properties of caseins at oil/water interfaces have also been widely studied, an area where the drop tensiometer technique has been extensively used.[24,25] These studies have provided detailed information on β-casein layers on hydrophobic surfaces in aqueous media where a saturated monolayer is generally achieved. The individual molecules in the monolayer adsorb with their hydrophobic regions anchored to the surface, with their hydrophilic tail protruding extensively into the aqueous phase. Regarding κ-casein layers, most of the works previously cited suggest the formation of a continuous layer formed by micelle-like structures.

Lateral force microscopy (LFM) is a special implementation of AFM devoted to the study of the tribological properties of surfaces. In LFM, the lateral force exerted on an AFM probe sliding over a sample surface is measured.[26] As a consequence of the typical small size of AFM probes, friction can be measured at the nanoscale. This can be of special relevance for the study of emulsions due to the small size of droplets. LFM also allows simultaneous recording of the topography signal in an easy-to-implement way.[27] Another possibility is to perform quantitative friction measurements while ramping the applied normal force, a methodology known as friction force spectroscopy (FFS).[28] Two different kinds of probes are commonly employed in friction measurements. The first ones, that is, colloidal probes, consist of micrometer-sized particles glued to a lever.[29] These probes offer a well-known shape and surface chemistry. Moreover, due to their large contact area, lower pressures than those exerted with nanometer-sized tips can be applied. Friction measurements performed with colloidal probes have provided valuable information on the lubricating properties of systems such as adsorbed layers of polyelectrolytes,[30] of proteins,[31] and even of complex films of biological molecules.[32,33] Nanometer-sized tips are the other type of probes typically used for friction measurements. Even though the precise shape of these probes is not well-known, they allow exerting very high pressures, so that not only the friction but also the wear of surfaces can be studied. Moreover, these tips also allow registering the topography of the sample during a friction measurement, so that changes in both parameters can be related. This technique has been successfully applied to the study of systems such as lipids[34,35] and protein layers.[27]

In this work, FFS was applied to study the tribological properties of β- and κ-casein layers at hydrophobic surfaces in aqueous solutions. These systems were chosen because of their relevance for protein stabilized systems, and also to determine if the FFS technique was sensitive to differences in the frictional/cohesive properties originating from the different chemical composition of the casein hydrophilic moieties. Oil/water interfaces would have been more relevant to study the emulsifying properties of caseins. However, these interfaces present different problems for AFM studies mainly because of their softness. To avoid these problems, sophisticated setups are needed.[36] In order to avoid these complications, we have used hydrophobized silica as a substrate. Nanometer-sized imaging tips were employed, so that topography and friction could be simultaneously measured on these surfaces. The results obtained are highly relevant describing the cohesive properties of the casein layers relevant to their use as dispersing agents and validate FFS as a powerful technique for the mechanical characterization of protein layers in liquid medium.

2. Materials and Methods

2.1. Proteins and Chemicals. β-Casein (product no. C6905) and κ-casein (product no. C0406) were purchased from Sigma Corp. and used without further purification. The dry protein samples were dissolved in water to a concentration of 0.2 $mg \cdot mL^{-1}$, giving a pH of the final solutions of 5.8 and 5.9 for β- and κ-casein, respectively. The purity of both protein solutions was determined to be over 85% by SDS-PAGE (Supporting Information section S1). The proteins were almost calcium-free as determined by atomic adsorption (OPTIMA 3000, Perkin-Elmer Co., Norwalk, CT), specifically 2×10^{-6} $mol \cdot mL^{-1}$ and 1.7×10^{-6} $mol \cdot mL^{-1}$ for 0.2 $mg \cdot mL^{-1}$ in water β- and κ-casein solutions, respectively. This corresponds to 0.24 moles of calcium per mole of β-casein, and 0.17 moles of calcium per mole of κ-casein. All other chemicals were of analytical grade or better. Water was treated by using a purifying unit (ELGA UHQ PS, Elga Ltd. U.K.) until a resistivity of 18 $M\Omega \cdot cm$ was attained.

2.2. Hydrophobization of Silica Surfaces. P-Doped (boron) silicon wafers with a resistivity of $10-20$ $\Omega \cdot cm$ (Semiconductor Wafer Inc., Taiwan) were oxidized in an oxygen atmosphere to obtain an oxide layer of approximately 30 nm.[37] Prior to hydrophobization, the silica (Si/SiO_2) substrates were cleaned as described elsewhere.[38] The clean silica surfaces were then hydrophobized by liquid-phase silanization. Specifically, the surfaces were dried in nitrogen gas and immersed in a solution containing 25 μL of dichlorodimethylsilane (Sigma-Aldrich, Stockholm, Sweden) and 50 mL of trichloroethylene for 1 h. After silanization, the surfaces were sonicated three times in trichloroethylene and three times in ethanol. The water contact angle after hydrophobization was determined to $95° \pm 5°$. The surfaces were stored in ethanol until use.

2.3. Sample Preparation. A volume of 50 μL of the casein solution was pipetted onto an hydrophobic silica surface and allowed to stand for 40 min. Samples were gently rinsed with water to remove any loosely associated material, taking care not to allow them to dry at any moment. Samples were then immediately placed on the microscope.

2.4. AFM. AFM measurements were performed with a commercial setup equipped with a liquid cell (Picoforce multimode SPM with a Nanoscope IV control unit, Veeco Instruments, Santa Barbara, CA). Rectangular silicon nitride levers with a nominal normal spring constant of 0.1 $N \cdot m^{-1}$ were employed in all the experiments (OMLC-RC800PSA, Olympus, Japan). The normal, k_N, and torsional, k_Φ, spring constants were determined for every lever using the methods developed by Sader and co-workers[39,40]

(22) Bantchev, G. B.; Schwartz, D. K. *Langmuir* **2004**, *20*, 11692–11697.
(23) Fang, Y.; Dalgleish, D. G. *J. Colloid Interface Sci.* **1993**, *156*, 329–334.
(24) Girardet, J. M.; Debomy, L.; Courthaudon, J. L.; Miclo, L.; Humbert, G.; Gaillard, J. L. *J. Dairy Sci.* **2000**, *76*, 2410–2421.
(25) Maldonado-Valderrama, J.; Gálvez-Ruiz, M. J.; Martín-Rodríguez, A.; Cabrerizo-Vílchez, M. A. *Langmuir* **2004**, *20*, 6093–6095.
(26) Binnig, G.; Quate, C. F.; Gerber, Ch. *Phys. Rev. Lett.* **1986**, *56*, 930–933.
(27) Bhushan, B.; Kwak, K. J.; Gupta, S.; Lee, S. C. *J. R. Soc., Interface* **2008**, *6*, 719–733.
(28) Meyer, E.; Lüthi, R.; Howald, L.; Bammerlin, M.; Guggisberg, M.; Güntherodt, H. J. *J. Vac. Sci. Technol., B* **1996**, *14*, 1285–1288.
(29) Ducker, W. A.; Senden, T. J.; Pashley, R. M. *Nature* **1991**, *353*, 239–241.
(30) Raviv, U.; Glasson, S.; Kampf, N.; Gohy, J. F.; Jerome, R.; Klein, J. *Nature* **2003**, *425*, 163–165.
(31) Hahn-Berg, I. C.; Liselott, L.; Arnebrant, T. *Biofouling* **2004**, *20*, 65–70.
(32) Hahn-Berg, I. C.; Rutland, M. W.; Arnebrant, T. *Biofouling* **2003**, *19*, 365–369.
(33) Cardenas, M.; Valle-Delgado, J. J.; Hamit, J.; Rutland, M. W.; Arnebrant, T. *Langmuir* **2008**, *24*, 7262–7268.
(34) Oncins, G.; Garcia-Manyes, S.; Sanz, F. *Langmuir* **2005**, *21*, 7373–7379.
(35) Oncins, G.; Torrent-Burgues, J.; Sanz, F. *Tribol. Lett.* **2006**, *21*, 175–184.
(36) Gonçalves, R. P.; Agnus, G.; Sens, P.; Houssin, C.; Bartenlian, B.; Scheuring, S. *Nature Methods* **2006**, *3*, 1007–1012.
(37) Wahlgren, M.; Arnebrant, T. *J. Colloid Interface Sci.* **1990**, *136*, 259–265.
(38) Svensson, O.; Arnebrant, T. *J. Colloid Interface Sci.* **2010**, *344*, 44–47.
(39) Sader, J. E.; Chon, J. W. M.; Mulvaney, P. *Rev. Sci. Instrum.* **1999**, *70*, 3967–3969.
(40) Green, C. P.; Lioe, H.; Cleveland, J. P.; Proksch, R.; Mulvaney, P.; Sader, J. E. *Rev. Sci. Instrum.* **2004**, *75*, 1988–1996.

and the AFM Tune IT software (ForceIT, Sweden). The lateral sensitivity of the setup, δ_Φ, was determined by the pivot method,[41] while the normal sensitivity, δ_N, was calculated from the slope of the deflection of the lever while pressed against a hard silicon surface. Moreover, the tips were rubbed against these surfaces to remove asperities from the apex. All levers were plasma cleaned for 5 min before being employed.

Friction measurements were performed by scanning the samples in the contact operation mode, that is, applying a constant load force during each scan. Typically, parallel lines along a square 2 μm × 2 μm area were scanned in opposite directions at a constant tip velocity of 16 $\mu m \cdot s^{-1}$. The fast scan direction was perpendicular to the long axis of the lever. For each scan, the topography and lateral force images were simultaneously recorded in both the trace and retrace directions. Images recorded consisted of 128 points in the fast scan direction (columns) and 32 points in the slow scan direction (rows). The number of rows was chosen as the minimum value for which all the material within the probed area could be removed; that is, no material was left between the scanned lines. The scan mean friction force was calculated by the following procedure: (i) first an inner square area, with a lateral size half of the scanned one, was selected for successive calculations in order to avoid border effects, (ii) the difference in the lateral signal between the trace and retrace directions, $\Delta V_{Lateral}$, was calculated for each scanning line, (iii) $\Delta V_{Lateral}$ was then averaged over all the lines of the images, and (iv) finally, the scan total friction force, F_F, was obtained by scaling $\Delta V_{Lateral}$ through the following equation:

$$F_F(\Delta V_l) = \frac{k_\Phi}{\delta_\Phi}\frac{1}{h_{eff}}\frac{\Delta V_{Lateral}}{2} \quad (1)$$

where h_{eff} is the effective height of the probe. For each scan, the load force applied by the lever, F_L, and the total normal force applied on the sample, F_N, were determined using the relationships:

$$\begin{aligned} F_N &= F_L + F_{adh} \\ F_L &= k_N\delta_N(V_{Vertical} - V_{Vertical\,0}) \end{aligned} \quad (2)$$

where $V_{Vertical}$ and $V_{Vertical\_0}$ are the photodiode vertical signals measured when the tip applies the load and when tip and sample do not interact, respectively. F_{adh} is the adhesion force between the tip and the sample. In order to minimize drift effects, a minimum of 30 min stabilization time was introduced between tip immersion, or solution exchange, and AFM measurements. Moreover, before each scan, the exact F_{adh} and $V_{Vertical\_0}$ values were determined by performing force curves on the sample. Force curves were acquired by displacing the sample over a vertical distance of 200 nm, at a velocity of 370 $nm \cdot s^{-1}$, while registering the vertical signal on the photodiode, $V_{Vertical}$. Conversion of force curves into force versus tip−sample distance curves was done as explained elsewhere.[42] Friction was characterized by friction−load curves, that is, plots of friction forces measured for a set of 2D scans performed at an increasing and/or decreasing set of load force values.

Analysis of AFM data was performed using self-programmed routines written in Matlab (Math Works Inc., Natick, MA). Topography images were represented with the WSxM software.[43]

2.5. Ellipsometry. The adsorption of β- and κ-casein to hydrophobized silica surfaces was monitored in situ by ellipsometry to obtain time-resolved values of the thickness and refractive index of the films in water. Theoretical principles can be found elsewhere,[44] and the experimental setup is based on null ellipsometry according to the principles of Cuypers.[45] The instrument used was a Rudolph thin film ellipsometer (type 43603-200E, Rudolph Research, USA), automated according to the concept of Landgren and Jönsson.[46] A xenon arc lamp was used as the light source, and light was detected at 442.9 nm using an interference filter with UV and infrared blocking (Melles Griot, The Netherlands). The trapezoid cuvette made of optical glass (Hellma, Germany) was equipped with a magnetic stirrer and thermostatted to 25 °C. A casein stock solution was added to the cuvette containing the surface immersed in 5 mL of water, and the adsorption was then monitored for 90 min followed by rinsing during 5 min.

The determination of the silicon complex refractive index, and of the thickness and refractive index of the silicon oxide layer, was performed using air and water as ambient media.[46] Four zone measurements were conducted to minimize systematic errors. The adsorbed amount was calculated from the refractive index and thickness of the protein film. For this, a linear increase for the refractive index with the concentration of 0.18 $mL \cdot g^{-1}$ was assumed.[47]

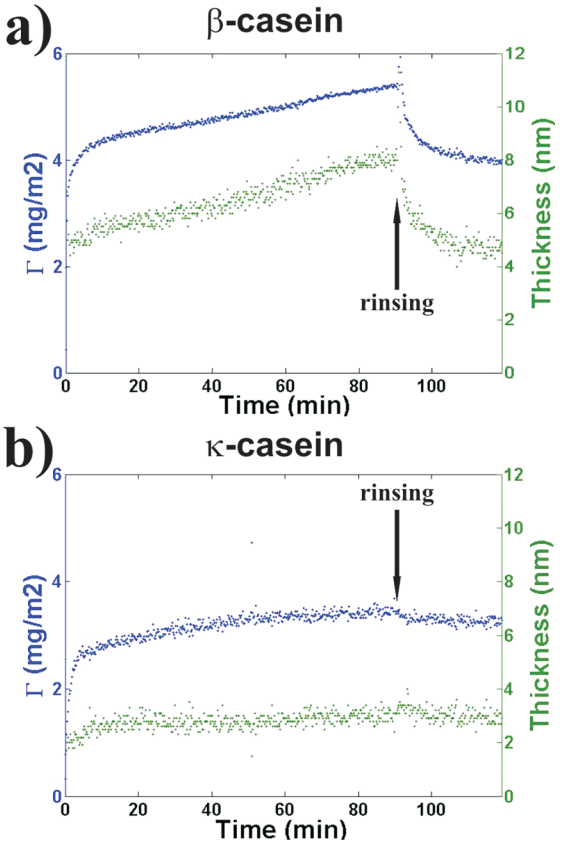

Figure 1. Time evolution of surface excess and layer thickness of (a) β-casein and (b) κ-casein layers determined by null-ellipsometry. Measurements were done in water. During the initial part of the experiments, the surfaces were incubated in a 0.2 $mg \cdot mL^{-1}$ protein solution. After an incubation time of 90 min, the surfaces were rinsed with water.

3. Results

3.1. Ellipsometry Study of the Formation of Casein Layers. The formation of casein layers on hydrophobized silica

(41) Bogdanovic, G.; Meurk, A.; Rutland, M. W. *Colloids Surf., B* **2000**, *19*, 397–405.
(42) Butt, H. J.; Cappella, B.; Kappl, M. *Surf. Sci. Rep.* **2005**, *59*, 1–152.
(43) Horcas, I.; Fernandez, R.; Gomez-Rodriguez, J. M.; Colchero, J.; Gomez-Herrero, J.; Baró, A. M. *Rev. Sci. Instrum.* **2007**, *78*, 013705.
(44) Azzam, R. M. A.; Bashara, N. M. *Ellipsometry and Polarized Light*; North-Holland: Amsterdam, 1977.
(45) Cuypers, P. A. *Dynamic ellipsometry: Biochemical and biomedical applications*; Ph.D. Thesis, Rijksuniversiteit Limburg: 1976.
(46) Landgren, M.; Jönsson, B. *J. Phys. Chem.* **1993**, *97*, 1656–1660.
(47) de Feijter, J. A.; Benjamins, J.; Veer, F. A. *Biopolymers* **1978**, *17*, 1759–1763.

surfaces has been studied by means of ellipsometry. Figure 1 shows the time evolution of the surface excess, Γ, and the mean thickness during the adsorption in water and subsequent rinsing of β- and κ-casein (Figure 1a and b respectively). In both cases, protein concentration during adsorption was 0.2 mg·mL^{-1} and rinsing started after 90 min. Both proteins show a fast initial adsorption. If we denote the final surface excess after rinsing by Γ_p, a relative surface coverage, $\Phi = \Gamma/\Gamma_p$, higher than 0.8 is achieved for β-casein within 1 min of incubation. However, soon after this point a steady-state increment of the coverage of about 0.015 mg·m^{-2}·min^{-1} is observed. After rinsing with water, the total amount of adsorbed protein was $\Gamma_p \approx 4$ mg·m^{-2}. The initial rate of adsorption is slightly slower for κ-casein, reaching $\Phi = 0.8$ after an incubation time of ~2.5 min. From this point, the increase of the coverage, of about 0.007 mg·m^{-2}·min^{-1}, is slower than in the case of β-casein. Moreover, after rinsing, a value of $\Gamma_p \approx$ 3.3 mg·m^{-2} is achieved.

3.2. Normal Forces on Casein Surfaces. Even though this work focuses on friction studies on casein layers, normal force curves have also been obtained on these systems. This has allowed gaining some insight both on the structure of these layers and on their conformation during friction measurements. Moreover, normal forces also give information on the quality of both sample and probe surfaces and therefore on the validity of friction measurements. Specifically, results are shown for the interaction between a silicon nitride AFM tip, the same type as those used to measure friction, and β- and κ-casein layers on hydrophobized silica substrates in a set of solutions of different ionic strengths: in water pH 5.9, in 10 mM NaCl pH 5.5, in 50 mM NaCl pH 5.5, and in 10 mM $MgCl_2$ pH 6.1. As a control experiment, normal forces were also probed when approaching the bare hydrophobic substrates (Supporting Information section S2). Force curves for this situation show an attractive interaction upon approach starting from a separation of about 5 nm. Interestingly, the distance range of this interaction does not seem to depend on the ionic strength of the surrounding solution. This further indicates a low density of charged groups in the hydrophobic surfaces.

Figure 2a shows force curves performed on top of a β-casein layer. The curve in water shows a long-range attractive force which starts at a distance of ~10 nm. When a small amount of monovalent ions is added (solution changed to 10 mM NaCl), the range of the attractive force is reduced to approximately half of its previous value, while a subtle longer range repulsive force appears. Fitting the repulsive part of several curves from the same set to an exponential function gives a characteristic length of 5.5 ± 1 nm. At higher ionic strength, as shown in Figure 2a with force curves obtained in 50 mM NaCl and in 10 mM $MgCl_2$, the range of the repulsive force is shortened (fits of curves from the same sets to exponential functions give characteristic lengths of 2.4 ± 0.6 nm and 2.1 ± 0.9 nm, respectively), while the attractive term is no longer observed. The force curves in Figure 2b were performed on a κ-casein layer. In water, the interaction is governed by an attractive force extending up to distances of ~10 nm. In 10 mM NaCl, the attractive force has practically vanished, while a smoothly decaying longer range repulsive force is observed. At higher ionic strengths, force curves in 50 mM NaCl and 10 mM $MgCl_2$ show that the repulsive force is still present. However, as observed for β-casein layers, the range of this force is confined within much shorter distances. Exponential fitting of the repulsive part of several force curves from the same experiment gives characteristic lengths of 6.9 ± 2.4 nm for 10 mM NaCl, 3.4 ± 1.0 nm for 50 mM NaCl, and 2.7 ± 0.8 nm for 10 mM $MgCl_2$. It is worth noting that, in the case of β- and κ-casein layers, the characteristic lengths obtained for the repulsive

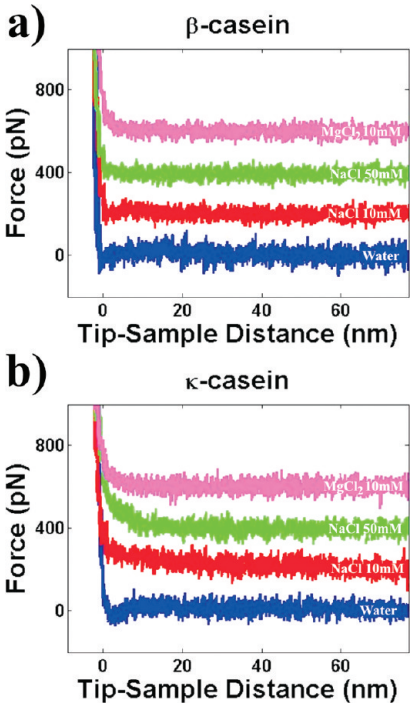

Figure 2. Normal force versus tip−sample distance curves corresponding to a silicon nitride tip probing (a) a β-casein layer and (b) a κ-casein layer in various solutions with different ionic strengths. Each of the represented set of curves was obtained with the same tip in order to minimize effects from differences in the probe surface. The force axes are not absolute scales but relative ones as, for each curve, the zero force corresponds to the average value measured far from the sample.

interactions are higher than those expected from the linearized Poisson−Boltzmann theory for a pure electrostatic interaction (i.e., Debye length, 3.04 nm for 10 mM NaCl, 1.36 nm for 50 mM NaCl, and 1.76 nm for 10 mM $MgCl_2$).[48] This will be further addressed in the Discussion section.

The curves in Figure 2 represent the typical tip−sample interaction (measured on approach) for casein monolayers. The exact magnitudes of the surface forces were subject to a slight variation between different tips, although usually below a factor 2, which is expected from the variable size and shape of the employed tips. By contrast, the extension and separation-length dependence of normal forces measured in our experiments were not subjected to a high variation, being similar to those of the presented curves. However, the tip−sample interaction can suffer drastic changes during a friction measurement due to tip modification/contamination. This also induced modifications on the measured friction−load curves. In order to avoid the evaluation of this data, force curves were performed before and after each friction measurement. Only in the case that these curves corresponded to those in Figure 2, the friction data was considered for further evaluation.

It can be observed from the curves in Figure 2 that the magnitude of the tip−sample surface forces in any of the presented situations is not much higher than ~100 pN. These forces are about 1 order of magnitude smaller than those exerted during friction measurements in this work (which are above 1 nN), indicating that they were performed with tip and sample in mechanical contact. Regarding the contact region of the curves, no indentation associated with rupture of the layers, even at the

(48) Sotres, J.; Baró, A. M. *Biophys. J.* **2010**, *98*, 1995–2004.

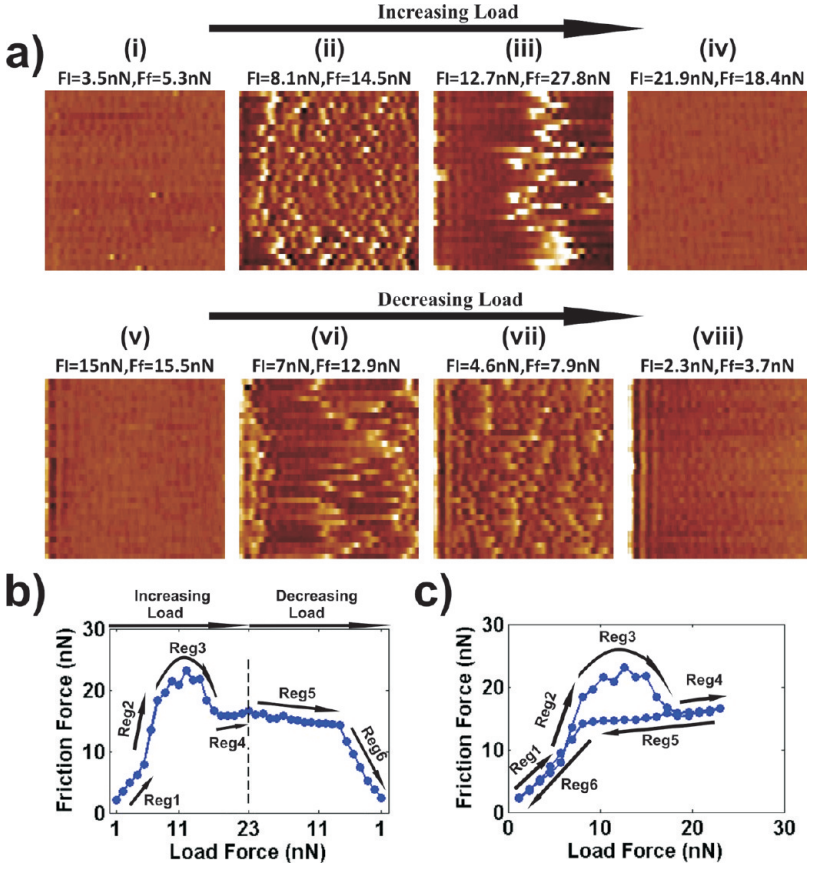

Figure 3. (a) Selected topography images corresponding to a friction measurement on a β-casein layer. Specifically, some characteristic processes of the friction measurement are represented: (i) Sliding of the tip along the protein layer. (ii) Indentation of the layer. (iii) Formation of protein aggregates. (iv, v) Visualization of the underlying silica substrate. (vi, vii, viii) Proteins diffusing back on the surface. (b, c) Two different representations of the friction−load curve for the friction measurement in (a). In (b), the friction forces for the increasing and for the decreasing load ramps are represented consecutively, while in (c) they are plotted within the same load force interval.

load forces applied during the friction measurements (range not shown in the figure), could be identified. The curves corresponding to tip−sample separation, not shown in Figure 2, did not display any appreciable adhesion. As a consequence, the applied load force could be directly associated with the total exerted normal force.

3.3. Friction Force Spectroscopy on Casein Monolayers. Friction on casein surfaces has been measured by successively scanning a given sample area while ramping the applied load between the scans. Specifically, two different ramps were applied, one of increasing loads followed by one of decreasing loads. A representative friction measurement on a casein layer is presented in Figure 3. It was performed on a β-casein layer, with a silicon nitride tip, in water environment. It will also be shown in the following sections that qualitatively similar data is obtained for different ionic strengths and pHs, and also for κ-casein layers. Figure 3a shows some selected topography images of the casein surface during the friction measurement. Representative profiles from simultaneously recorded lateral force images are shown in the Supporting Information section S3. The corresponding friction−load curve is shown, in two different representations, in Figure 3b and c. In Figure 3b, the friction forces for the increasing and for the decreasing load ramps are represented consecutively. In Figure 3c, the friction forces for both ramps are represented within the same load force interval.

Different regimes or patterns are highlighted in the friction−load curves of Figure 3. These regimes are representative for the processes depicted in Figure 3a. At the beginning of the increasing load ramp, two different regimes with a linear response of the friction force are observed. In the first one, Reg1, the compact protein layer is probed. This can be inferred from the homogeneous signals of the corresponding topography, Figure 3a(i), and of the lateral forces (Supporting Information section S3). Increasing the load leads to a different linear regime (Reg2). It is characterized by the applied force being high enough for indenting the layer, but not for removing it completely, Figure 3a(ii). There is a local increment in the lateral force associated with the indentation of the layer (Supporting Information section S3). Moreover, the frequency of indentation also increases with the load. These two factors lead to the observed increase in the slope of the friction−load curve, from now on friction coefficient, with respect to the previous regime. At higher load forces, a nonlinear friction regime appears (Reg3) where an initial increase followed by a posterior decrease of the friction force is observed. This regime is characterized by the visualization of protein aggregates with heights up to 20 nm, Figure 3a(iii). While the lateral forces exerted by the aggregates increase with load, their number decreases as more of them are pushed away from the scanning area. A further increase in the load force leads to a new friction regime (Reg4) characterized by the complete removal of the aggregates and by the visualization of the bare underlying silica substrate, Figure 3a(iv). In this regime, the friction force increases again linearly with the load, exhibiting the lowest friction coefficient of the whole friction−load curve. Decreasing the load from this point leads to a friction regime (Reg5) with a similar friction coefficient as the previous one, and where the underlying silica

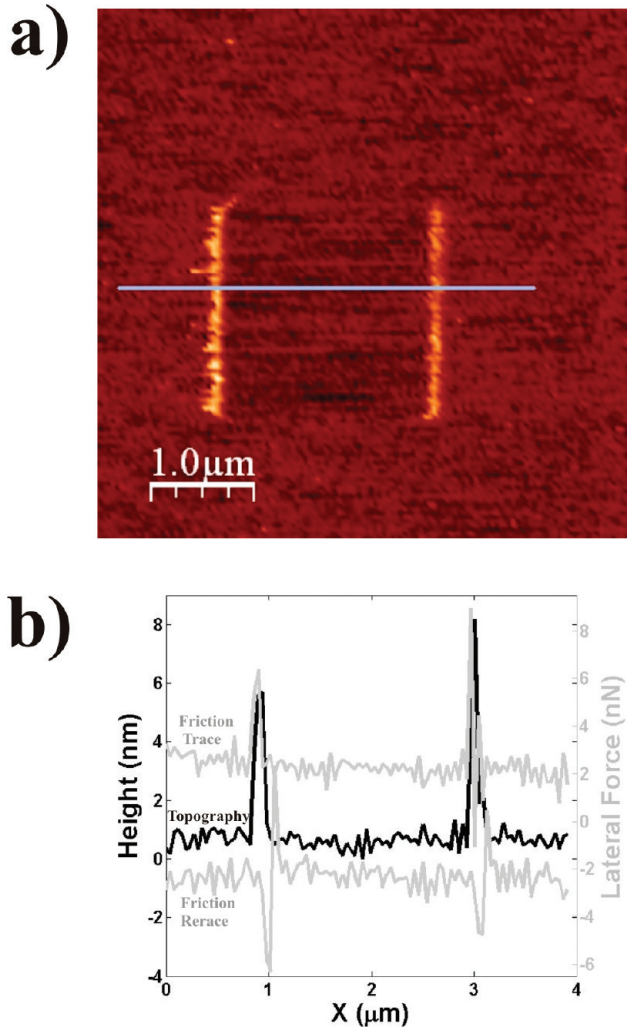

Figure 4. (a) AFM topography image obtained in the contact mode showing a β-casein layer just after an inner area of the image was scratched (that between the rows of removed material). (b) Superposed profiles of height and friction force for the trace and retrace directions corresponding to the scan line highlighted in (a).

substrate is also visualized, Figure 3a(v). It extends down to loads similar to those for which aggregates appeared while increasing the load. At even lower loads (Figure 3a(vi), (vii), and (viii)), the recovering of the protein coverage is observed. A final friction regime (Reg6) is defined by this process, with the friction coefficient being similar to that of Reg1.

The presented data suggests that the casein molecules diffuse back over the probed surface area, so that the full protein coverage is recovered. This was confirmed by imaging the surfaces after the friction measurements at very low loads. Figure 4a shows a topography image, obtained at a load force of ~0.1 nN, of the same β-casein layer as in Figure 3. The image was obtained immediately after the friction measurement, where the probed area was the one in between the columns of the removed material. In Figure 4b, superimposed profiles for the topography and lateral forces in opposite directions are shown for the scan line highlighted in Figure 4a. Similar values are observed for the height and the lateral force signals inside and outside the previously scratched area, confirming the recovery of the protein layer.

3.4. Analysis of Friction−Load Curves: Comparison between β- and κ-Casein Layers. Three different friction−load curves performed with the same tip on a clean hydrophobized

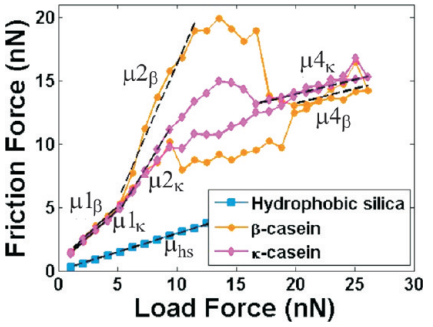

Figure 5. Friction−load curves represented in the same way as in Figure 3c. Curves correspond to friction measurements performed with a clean silicon nitride tip of a β-casein layer (circles), of a κ-casein layer (diamonds), and of a clean hydrophobic silica surface (squares). Linear fits of the different friction regimes are shown as dashed lines.

Table 1. Friction Coefficients for the Different Regimes Depicted in Figure 5[a]

β-casein	κ-casein	hydrophobic silica
$\mu 1_\beta = 1.02 \pm 0.18$	$\mu 1_\kappa = 0.96 \pm 0.16$	$\mu_{hs} = 0.22 \pm 0.06$
$\mu 2_\beta = 2.83 \pm 1.08$	$\mu 2_\kappa = 1.88 \pm 0.58$	$\mu_{hs} = 0.22 \pm 0.06$
$\mu 4_\beta = 0.22 \pm 0.18$	$\mu 4_\kappa = 0.24 \pm 0.08$	$\mu_{hs} = 0.22 \pm 0.06$

[a] Mean and standard deviation values from five experiments are presented.

silica surface, on a β-casein layer, and on a κ-casein layer are presented in Figure 5. While a simple linear friction behavior is observed for the hydrophobic silica surface, the friction−load curves on the casein layers show the same friction regimes as the one in Figure 3. All these regimes, except Reg3, show a linear dependence of friction with load. Thus, they can be characterized by their friction coefficient. As seen in Figure 5, it is reasonable to assume that the regimes for low applied load forces, Reg1 and Reg6, share the same friction coefficient which we denote by $\mu 1$. A similar assumption can be made for Reg4 and Reg5, denoting their friction coefficients by $\mu 4$. Finally, the friction coefficients for Reg2 and for the hydrophobized silica substrate are denoted by $\mu 2$ and μ_{hs}, respectively.

Mean and standard deviation error values for the different friction coefficients are presented in Table 1. These values were obtained by averaging five friction−load curves performed with different tips. The relatively low errors indicate that the friction coefficient can be considered as a highly tip-independent parameter. At low applied load forces, similar friction forces and coefficients are observed for the two studied protein surfaces ($\mu 1_\beta \approx \mu 1_\kappa$). It is noticeable that the force from where the layers start to be indented, and which sets the beginning of Reg2, is also similar for both systems. The friction coefficients for this regime are increased by a factor 2−3 with respect to those of Reg1. Furthermore, the one for β-casein, $\mu 2_\beta$, almost doubles the one for κ-casein, $\mu 2_\kappa$. The friction coefficients of Reg4 for β- and κ-casein layers, $\mu 4_\beta$ and $\mu 4_\kappa$, respectively, are almost identical between them and also when compared to that of clean hydrophobized silica, μ_{hs}.

The regime of the friction−load curves characterized by the formation of protein aggregates, Reg3, cannot be assigned a constant friction coefficient due to its curved shape. Instead, to characterize this regime, we have used the maximum of the friction−load curve prior to complete protein removal. The total force applied in this point, F_{Max}, is calculated by adding the corresponding load, F_{MaxL}, and friction, F_{MaxF}, components.

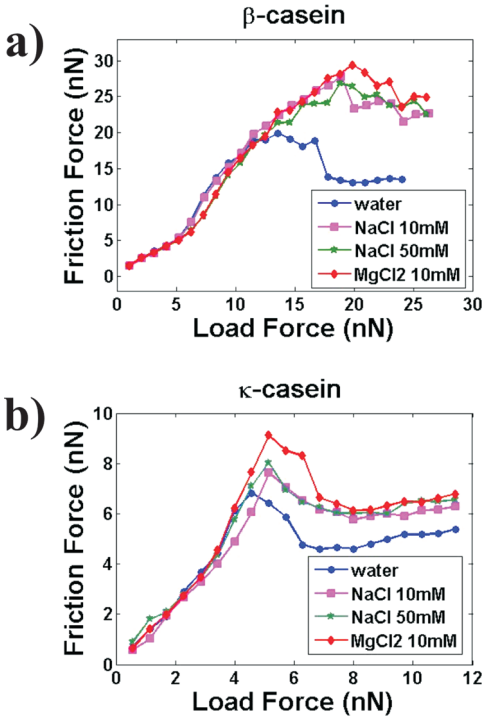

Figure 6. Friction−load curves for a silicon nitride tip probing (a) a β-casein layer and (b) a κ-casein layer in water, NaCl 10 mM, NaCl 50 mM, and $MgCl_2$ 10 mM.

Even though the value of F_{Max} varied between tips, we have found that the ratio between F_{Max} values measured for two different systems with the same tip was almost a tip-independent parameter. This ratio, from now on referred as relative cohesion, between two different systems A and B is given by:

$$r_{B/A} = \frac{(F_{max})_B}{(F_{max})_A} = \frac{\left(\sqrt{F_{maxL}{}^2 + F_{maxF}{}^2}\right)_B}{\left(\sqrt{F_{maxL}{}^2 + F_{maxF}{}^2}\right)_A} \qquad (3)$$

A value of $r_{\beta/\kappa} = 1.4 \pm 0.3$ has been obtained after averaging results from three different measurements, for the relative cohesion between β- and κ-casein layers in water. This result indicates that the total force needed to remove the protein layer, and thus its cohesion, is higher for β-casein than for κ-casein. The relatively low errors found when averaging relative cohesions results from different tips prove it as an almost tip-independent parameter.

3.5. Casein Layers Friction Dependence with pH and Electrolyte Concentration. The dependence of the friction properties of β- and κ-casein layers with electrolyte concentration has been studied through friction−load curves performed on both systems in water pH 5.9, NaCl 10 mM pH 5.5, NaCl 50 mM pH 5.5, and $MgCl_2$ 10 mM pH 6.1. Examples are shown in Figure 6a for β-casein and in Figure 6b for κ-casein. All of the curves from each of the figures were obtained with the same tip. It can be observed that neither the friction coefficients of the different regimes nor the transition force between regimes 1 and 2 show any dependence with the electrolyte concentration. By contrast, it is clear that the maximum friction force exerted before protein removal increases when electrolytes are added to the solution. To quantify this behavior,we have measured the relative cohesion between casein layers probed in a given electrolyte solution and in water ($r_{solution/water}$ as defined by eq 3). Average values of this parameter in different solutions are presented in Table 2 for both β- and κ-casein layers. While higher layer cohesion at higher ionic

Table 2. Relative Cohesion Measured between Friction−Load Curves Performed Both in a Given Electrolyte Solution and in Water[a]

	$r_{NaCl\_1mM/water}$	$r_{NaCl\_10mM/water}$	$r_{MgCl_2\_10mM/water}$	$r_{PBS/water}$
β-casein	1.2 ± 0.2	1.3 ± 0.3	1.4 ± 0.2	0.6 ± 0.2
κ-casein	1.2 ± 0.2	1.2 ± 0.2	1.3 ± 0.3	0.7 ± 0.2

[a] Mean and standard deviation values from three experiments are presented both for and for β- and κ-casein monolayers.

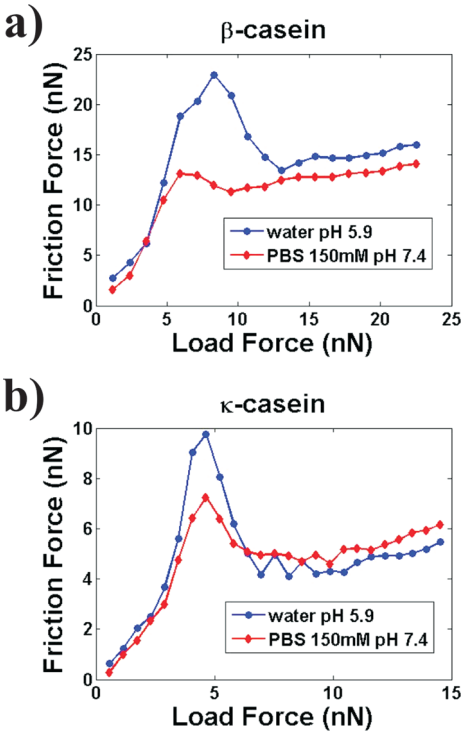

Figure 7. Friction−load curves for a silicon nitride tip probing (a) a β-casein layer and (b) a κ-casein layer both in water pH 5.9 and in PBS 150 mM pH 7.4.

strengths can be concluded for both protein surfaces, it is difficult to determine from these results if the cohesion of the layers shows any specificity for the valence of the ions present in the solution. Moreover, electrolyte concentration is not the only characteristic from the solution that induces detectable variations in the friction response of casein layers. The pH of the solution also has a noticeable influence. Friction−load curves performed in water pH 5.9 and in PBS 150 mM pH 7.4 buffer are presented in Figure 7a and b for β- and κ-casein respectively. From the previous results, an increase in the cohesion of the layers would be expected when changing the solution from water to PBS. However, as seen in Figure 7 and in the average relative cohesion values presented in Table 2, an opposite behavior is detected. Thus, this decrease in the cohesion of the layers has to be a consequence of the increase in pH.

3.6. Funicity Study of Casein Layers. For the study of funicity, that is, the dependence of friction forces on previous history,[49] several friction−load curves were measured sequentially on the same area of casein surfaces. Examples are shown in Figure 8a and b for a sequence of three friction−load curves performed in water on β- and κ-casein layers, respectively. In both cases, the second curve was performed just after the first one, while the third was performed after 30 min. The first friction

(49) Urbakh, M.; Klafter, J.; Gourdon, D.; Israelachvili, J. *Nature* **2004**, *430*, 525–528.

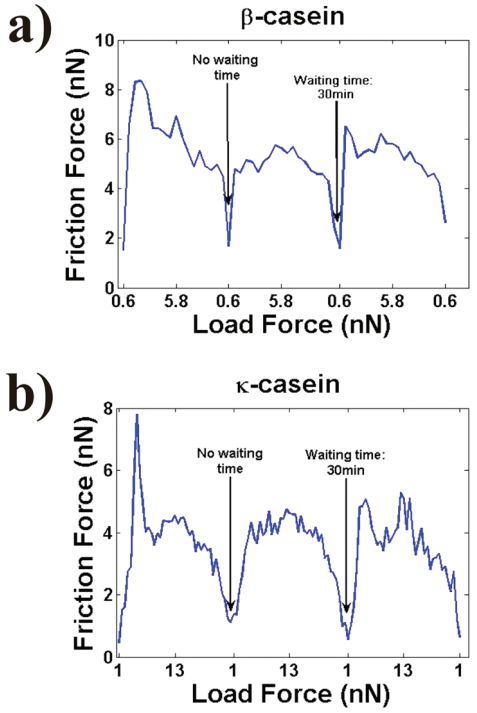

Figure 8. Friction−load curves for three consecutive scratches of the same area of (a) a β-casein surface and of (b) a κ-casein surface.

shows, both for β- and κ-casein layers, the same regions described in section 3.3. By contrast, the curves performed in second place do not show the curved pattern, Reg3, associated with the presence of protein aggregates. Interestingly, Reg3 is observed again for the friction−load curves performed in the same area after a stabilization time of 30 min. This behavior was fully reproducible when scratching different zones of the samples.

3.7. Measurement and Analysis of Wear in Casein Layers. The experimental procedure used for the study of friction also offers the possibility of studying wear. Usually, the study of wear is approached by measuring the volume worn while scratching a sample at different applied loads. These magnitudes can be related by the Archard equation[50] which states that the worn volume, V_w, along a line of length l applying a load force F_L is given by

$$V_w = K_w l F_L \quad (4)$$

where K_w is the effective coefficient of wear. However, eq 4 cannot be directly applied to interpret our experimental data since V_W is not an experimentally measured magnitude. However, it can be expressed as the difference between the initial volume, V_0, and the residual volume after completing each scan, V_{res}, so that $V_W = V_0 - V_{res}$. V_0 is defined as a constant. V_{res} can be calculated after each 2D scan by integrating the registered height data over the scanned area (Figure 9a). For this, the height of the underlying silica substrate is chosen as a reference zero value. This is a requirement that implies that V_{res} can only be calculated for scans where the clean substrate is clearly identified. Another problem in applying eq 4 is that 2D areas, and not straight lines, were scanned. We have overcome this difficulty by scaling V_W by the scan area, A, instead than by a scan length as in eq 4. This implies that the parameter relating the scaled worn volume to the applied load, the new efficient coefficient of wear for 2D scans K_{w2D}, will now represent the worn volume per unit area per unit load or,

(50) Archard, J. F.; Hirst, W. *Proc. R. Soc. London, Ser. A* **1956**, *236*, 397–410.

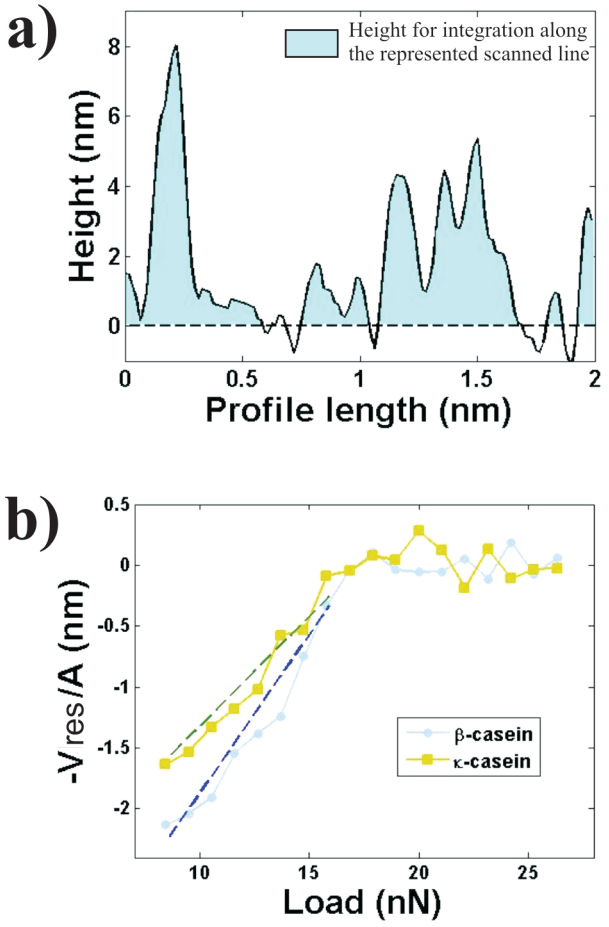

Figure 9. (a) Topography profile of a β-casein layer during a friction experiment. The filled area is the one used for volume integration. (b) Wear curves for two different friction experiments, performed with the same tip, on a β-casein layer (circles) and on a κ-casein layer (squares). Fits of both curves to eq 5 are also plotted (dashed lines).

more intuitively, the decrease in sample thickness per unit load. We are aware that this coefficient has complex dependences on different experimental parameters. Thus, it is not clear to which extent K_{w2D} could be compared with other wear coefficients more commonly found in the literature. However, it can be used for comparing the wear between the different systems studied in this work. Thus, the following expression is proposed for modeling wear in friction experiments:

$$\frac{-V_{res}}{A} = -\frac{V_0}{A} + K_{w2D} F_L \quad (5)$$

In Figure 9b, the scaled residual volume, $-V_{res}/A$, is plotted against the applied load for the same friction measurements as in Figure 5. From now on, this representation will be referred to as wear curves. Fits to eq 5 are also shown in Figure 9b. It is straightforward to obtain K_{w2D} for both systems, as it equals the slope of the linear fits. Moreover, the good fit obtained for both curves implies that it is reasonable to approximate K_{w2D} as a constant, at least within our experimental conditions. For the curves from Figure 9b, these coefficients are $K_{w2D(\beta\text{-casein})} = 0.26$ nm/nN and $K_{w2D(\kappa\text{-casein})} = 0.18$ nm/nN. Although the value of K_{w2D} varied between experiments performed with different tips, these values represent the general trend observed in our experiments. That is, κ-casein layers showed lower K_{w2D} than those of β-casein.

4. Discussion

Previous investigations on the adsorption of caseins on hydrophobic substrates have shown that both β- and κ-casein adsorb irreversibly with respect to rinsing with buffered solutions.[7,14,16] In these studies, the reported amount was between 2 and 3 mg/m^2 and the reported thickness around 5 nm. For β-casein (Figure 1a), we detect a higher surface coverage than that reported by others.[16] This surface excess can be attributed to a decrease in the intra- and intermolecular repulsion (a consequence of operating near the pI of the protein). In fact, if the adsorption of β-casein is followed at a higher pH (results for pH 7 shown in Supporting Information section S4), surface coverage values in excellent agreement with those reported by others[16] are obtained. Moreover, no sign of aggregates was seen in the topography images recorded along with the friction data (Supporting Information section S3). Therefore, it is reasonable to assume that the increase in adsorbed mass is due to a loosely adsorbed fraction of β-casein molecules on the surface and that they do not influence the friction measurements. Regarding κ-casein, individual molecules in solution are connected by disulfide bonds forming oligomers.[6] From electrophoresis data, it is clear that our sample apart from monomers also contains oligomers (data not shown). The oligomeric nature of κ-casein results in a decrease of the monomer concentration, and this is also reflected in the slower initial binding kinetics compared with β-casein (Figure 1).

From the thickness data, we propose that a monolayer is formed for both β- and κ-casein on the hydrophobized silica surface. Although, κ-casein partly exists as disulfide linked oligomers, we propose preferential adsorption of monomers due to their stronger amphiphilicity resulting in a monolayer formation. As presented in this study, both caseins are able to fill up the space/gaps created by the scratching process, which is explained by diffusion in the lateral plane of the surface. The lateral diffusion also implies that dense layers of caseins form on the surface, which is confirmed by our ellipsometric results. From the refractive indices of the films, the calculated volume fraction of protein in the films is close to 80%.

Useful information on the structure of casein layers can be inferred from normal force measurements. As seen in Figure 2, a similar tip−sample interaction is observed with both β- and κ-casein layers. Thus, the following analysis applies for both systems. When working in ionic solutions, the contribution of electrostatic double layer (EDL) forces to the total tip−sample interaction should be considered. At the pHs of the experiments, both the silicon nitride tip (pI between 2 and 3 due to the formation of a silicon oxide layer on the surface)[51] and the caseins (pIs of 4.5 and 4.1 for β- and κ-casein respectively)[52] are negatively charged. As a consequence, EDL forces between these surfaces are expected to be repulsive, in contrast to the attractive long-range force measured in low ionic strengths. Moreover, the repulsive component of the measured forces extends toward longer distances than those expected for an EDL interaction. Therefore, EDL interactions cannot be the only component of the measured forces. One could think about different origins for these observations. Tip−substrate hydrophobic interactions are unlikely to account for the observed attraction at low ionic strengths in the presence of casein layers. As shown in the Supporting Information section S2, the range and magnitude of the hydrophobic interaction does not significantly vary with the ionic strength, as opposed to the attraction observed when approaching the casein layers. Short range attractive forces between β-casein layers have been previously observed in magnetic chaining experiments.[53] However, these experiments were performed with β-casein present in solution and at a concentration higher than the critical micelle concentration. For this reason, the attraction was attributed to a depletion interaction originated by the presence of β-casein micelles in the measuring solution. However, this explanation cannot be applied to our results as our samples were rinsed after film formation and the force measurements were performed in protein-free solutions. As shown in the electrophoregrams of the Supporting Information section S1, the initial stocks of β- and κ-casein also contain a small amount of α_{s1}-casein. As commented in the Introduction, this protein has alternating hydrophobic and charged domains. Thus, its presence in the casein layer could cause attractive bridging interactions. However, we do not consider this as the origin of the measured attractive interaction. The reason is that the interaction was highly reproducible throughout the samples. During a normal force measurement, the AFM tip, due to its small size, will not interact with more than a few tens of casein molecules. Considering the reported homogeneity of the interaction throughout the samples, it should be assumed that a high portion of the layers would have to be composed of α_{s1}-casein for this molecule to originate the measured attraction at low ionic strengths. We consider this option improbable, not only because of the much higher amounts of β- and κ-casein in the corresponding initial stock solutions but also because it has been shown that β-casein, as a consequence of being more surface active (we expect a similar behavior for κ-casein), displaces α_{s1}-casein from layers formed at hydrophobic surfaces.[54] The presence of calcium ions in the initial protein solutions is so small (see Materials and Methods section 2.1) that it is very unlikely that they account for the measured attraction.

To understand the origin of the measured normal forces, it is necessary to consider the coil-like behavior of caseins. At low electrolyte concentrations, the molecules will extend throughout the aqueous medium. Indeed, thickness values of ~10−20 nm have been measured for β-casein monolayers in low ionic strength solutions.[14] This explains the long range of the measured surface forces. At low ionic strengths, the hydrophilic part of the molecules, which contains both positively and negatively charged residues, probably has the conformational freedom to orientate itself facing the negatively charged tip with its positive residues. This leads to the measured long-range attractive interaction. When the ionic strength of the medium is increased, it is expected that two different processes take place. First, the compaction of the molecules and the decrease of the range of the electrostatic interaction will lead to the observed reduction in the range of the surface forces. Second, the molecules will progressively lose their ability to reorient as a result of being more compacted, and the separation between the charged residues will be smaller. In this case, the tip will probe the net negative charge of the caseins, accounting for the purely repulsive force observed when increasing the ion concentration.

Normal force measurements also provide useful information to analyze friction data. First, it is clear from the normal force curves that, independent of the electrolyte concentration, the proteins are compressed under applied forces lower than those typical of friction experiments. Moreover, normal force curves, which are

(51) Lyklema, J. *Fundamentals of Interface and Colloid Science ii*; Academic Press: San Diego, 1995.
(52) Cordeschi, M.; Di Paola, L.; Marrelli, L.; Maschietti, M. *Biophys. Chem.* **2003**, *103*, 77–88.
(53) Dimitrova, T. D.; Leal-Calderon, F. *Langmuir* **1999**, *15*, 8813–8821.
(54) Dickinson, E.; Rolfe, S. E.; Dalgleish, D. G. *Food Hydrocolloids* **1988**, *2*, 397–405.

very sensitive to modifications/contaminations of the tips, were used for assuring the quality of friction data.

This work is mainly based on the use of friction−load curves to characterize friction on casein layers. These curves show different regimes (Figure 3), with each of them being representative of a distinct friction process. These regimes have been characterized by parameters such as the friction coefficient or the relative cohesion. The relatively low errors found for these parameters are an indicator of the high reproducibility of the friction−load curves and thus of the homogeneity of the casein layers. We first focus on the first regime, Reg1, characterized by the tip sliding over compact layers of caseins. The compressed nature of the layers is inferred both from normal force measurements and from the homogeneity of the topography and lateral force images. The friction coefficient of this regime is about ∼1 for both β- and κ-casein layers in the whole range of experimental conditions (electrolyte concentration and pH) studied. It is instructive to compare these coefficients with those of other systems. Typically, molecules known for their lubricating properties confer surfaces with lower fiction coefficients. Examples go from block copolymers ($\mu \sim 0.001$ when adsorbed on hydrophobic surfaces)[30] to natural biological lubricants such as as human whole saliva ($\mu \sim 0.03$ when adsorbed on hydrophilic surfaces),[32] PRP-1 ($\mu \sim 0.01$ on hydrophilic surfaces),[31] or lubricin ($\mu \sim 0.03$ when adsorbed on hydrophilic surfaces and $\mu \sim 0.3$ when adsorbed on hydrophobic surfaces).[55] Interestingly, the friction coefficients obtained when sliding the hydrophilic AFM tip against the casein surfaces resemble those reported for hydrophobic surfaces covered with nonionic surfactants ($\mu \sim 1$),[56] indicating that these systems constitute highly dissipative surfaces. As mentioned earlier, β- and κ-casein differ both in their net charge and in their degree of phosphorylation and glycosylation. However, it seems that none of these characteristics play an important role in the frictional properties of casein monolayers at low applied loads, as inferred from the similarity between friction coefficients.

When the load force is increased up to a value of ∼5 nN, the friction on both casein layers goes through a regime transition. The force from where this new regime, Reg2, is observed has been shown to vary between different tips, but not with the electrolyte concentration or pH of the medium. This regime is characterized by the tip starting to indent the layers. Just after an indentation event, the exerted lateral force has to be considerably increased to keep the tip sliding at a constant velocity. Moreover, the frequency of indentation is also incremented with the applied load. As a consequence, the friction forces are higher and increase with the load force at a rate 2−3 times than observed in the previous friction regime. This can be interpreted by considering that the force needed to indent the layers is not sufficient to keep removing them after the indentation. Thus, the tip becomes trapped, and a considerable increment in the exerted lateral force is needed to take the tip out from the indented hole. This process is extremely interesting when considering the protective properties of casein monolayers, as it implies that they have the ability to capture particles that provide sufficient force to penetrate them. The fact that the friction coefficient of this regime is higher for β-casein than for κ-casein is an indicator not only of a higher shear resistance but also of a higher layer cohesion.

At higher loads, a new friction regime is reached, Reg3, where the total applied force is high enough not only for indenting the casein layers but also for breaking through them while pushing the molecules away. In this situation, the removed molecules tend to aggregate. When the tip encounters these aggregates, it slides over them if the applied force is not sufficient to displace them. High lateral forces are associated with the sliding over these aggregates, being the origin of the high friction forces of Reg3. These forces indicate that the aggregates have both a high cohesion and a strong interaction with the hydrophobic substrate. Increasing the applied force along this regime has two main effects. On one hand, the friction force associated with the sliding over the aggregates increases. However, on the other hand, more aggregates are displaced at higher forces. Thus, their number decreases with the subsequent reduction in the overall friction force. These two processes are the origin of the curved shape of friction Reg3, which ends when the force is high enough to remove all the protein aggregates.

Our experimental results can be used to gain insight into the function of caseins as stabilizers of suspensions and emulsions. In order to explain this, we now compare our data with those reported from colloidal particle scattering (CPS) experiments, a technique that measures the sticking probability between particles/droplets after a collision induced by a hydrodynamic flow, being possible to control the force of the collision by controlling the shear rate of the flow chamber.[57] With this technique, it has been shown that micrometer-sized casein-stabilized particles/droplets have already a high probability of sticking together (coagulating) when they collide with forces in the order of $10^{-4}-10^{-5}$ nN.[58] It has been theoretically determined that, for this sticking to be possible, the presence of attractive/adhesive[59] or friction[60] forces that can oppose to the hydrodynamic driving force is needed. On one hand, it has been shown that, when the measuring solution contains even a small amount of salts, attractive/adhesive forces are not present on top of casein surfaces. On the other hand, our data does support the involvement of friction forces in the sticking between casein covered particles/droplets. Indeed, the observations from Semenova et al.[58] could be explained by assuming that the presented frictional response of casein surfaces can be extrapolated down to the forces applied in their experiments, that is, the presence of a friction force of a similar magnitude to that of the applied hydrodynamic force. One could also think of the rupture of the casein layer and subsequent direct hydrophobic interaction between the inner particles/droplets as a possible explanation for the sticking events. However, this is not consistent with our data. We can estimate the maximum pressure that can be exerted on casein monolayers before they are removed. For this, we consider a model spherical tip with a nominal radius of 20 nm and a model casein layer with a thickness of 3 nm. Our experiments show that the maximum friction force exerted on the layers is in the order of 20 nN. At this force, the layer can be considered fully indented by the tip. While sliding in this situation, it is estimated from geometrical considerations that a tip area, with a half spherical cap shape, of ∼190 nm^2 will be pushing the molecules, exerting a pressure of about 10^8 Pa. A similar calculus gives at hand that the pressure between two casein-covered spheres sticking together in the previously commented CPS experiments is in the order of 10 Pa. This value is several orders of magnitude smaller than that needed to break

(55) Zappone, B.; Ruths, M.; Greene, G. W.; Jay, G. D.; Israelachvili, J. N. *Biophys. J.* **2007**, *92*, 1693–1708.
(56) Graca, M.; Bongaerts, J. H. H.; Stokes, J. R.; Granick, S. *J. Colloid Interface Sci.* **2007**, *315*, 662–670.
(57) Murray, B. S.; Dickinson, E.; McCarney, J. M.; Nelson, P. V.; Whittle, M. *Langmuir* **1998**, *14*, 3466–3469.
(58) Semenova, M. G.; Chen, J.; Dickinson, E.; Murray, B. S.; Whittle, M. *Colloids Surf., B* **2001**, *22*, 237–244.
(59) Whittle, M.; Murray, B. S.; Dickinson, E. *J. Colloid Interface Sci.* **2000**, *225*, 367–377.
(60) Whittle, M.; Murray, B. S.; Chen, J.; Dickinson, E. *Langmuir* **2000**, *16*, 9784–9791.

the casein layer. Thus, our data proves not only the existence but also the important role of friction forces in the sticking between casein-covered particles/droplets, and subsequently the potential use of FFS to study the coagulating conditions of suspensions/emulsions.

Friction regime Reg3 is the most sensitive to both sample and experimental condition variations. The relative cohesion, that is, the ratio between the forces that have to be applied on both samples for complete protein removal (eq 3), has been proposed as a parameter to quantify these variations. Our results show that β-casein monolayers are about ~1.4 times more cohesive than κ-casein monolayers. The cohesion of both samples has also been proved to depend on the electrolyte concentration and on the pH of the surrounding medium. At a pH range of ~5.5−6, where both tip and sample surfaces are negatively charged, the cohesion of both protein layers was observed to increase with the electrolyte concentration. This can be explained by the electrostatic screening between the monomers being reduced by the presence of the ions. Despite the known affinity of caseins for calcium, the cohesion of the layers was not specially favored by the presence of divalent magnesium cations. This leads us to think that the specific ion effect of the involved cations could be an important parameter regarding their stabilizing/aggregating function. However, to verify such a statement, deeper studies are needed. It has also been shown that the cohesion is clearly reduced when the pH is increased up to a value of 7.4, even if the electrolyte concentration is simultaneously increased. This implies that the layers are more cohesive when probed at pHs closer to the pI of the proteins. The effects of both added electrolyte and change in pH indicate that a reduction in inter- and intramolecular electrostatic interactions will increase the cohesion of the layers. Interestingly, the cohesion of β- and κ-casein monolayers, despite being of different magnitudes, seems to have a similar dependence on the ionic strength or pH of the measuring solution. Again, this seems to be unexpected based on the different affinity of both proteins for calcium. However, normal force measurements (Figure 2) already showed a similar behavior of the electrostatic interaction for both type of layers. Therefore, it seems that, while the specific chemistry of the caseins determines the absolute cohesion of the layers, the changes in cohesion that accompany changes in the electrostatic properties of the measuring solution follow a similar pattern for both casein layers.

Furthermore, the relative cohesion has been shown to be dependent on the previous friction history of the sample. Specifically, a friction−load curve performed on a previously scratched area does not show the curved Reg3; that is, the big protein aggregates do not reappear while scratching. A layer stabilization time in the order of tens of minutes must be allowed in order for this regime to appear again. This suggests that the structure of the layers varies with time. It can be expected that the diffusion of molecules back onto the scratched surface area lasts for a much longer time period than that required to initially cover it. In this case, the concentration of proteins within this area will also continuously increase, ideally until its value equals that from the surrounding surface. Interestingly, two different conformations for β-casein molecules within a monolayer have been reported from enzymatic digestion experiments.[23] In this work, the factor determining the conformation was found to be the protein density in the monolayer. Following this idea, we suggest that the presence of aggregates is dependent on the density of proteins in the monolayers. If enough time elapses between two friction measurements, a conformational change is expected for the proteins within the probed area as their concentration increases progressively. In turn, this will induce a modification in the structure of the monolayer resulting in the measured increase in cohesion.

In a friction experiment, the applied load can be increased above the point where all the protein aggregates are removed. For both protein layers, this regime, Reg4, shows a similar linear dependence with the applied force (friction coefficient) as friction on clean hydrophobized silica surfaces. This implies that the tip−substrate interaction is the factor that dominates the dependence of friction with load within this regime. There is also a difference amounting to several nN between the friction forces measured at the same applied load on caseins friction, Reg4, and on the hydrophobic substrate. This can be explained by the fact that the molecules are diffusing back at a velocity which is faster than that of the friction measurements (which is in the order of $\mu m \cdot s^{-1}$), so that they are constantly surrounding the sliding tip. In this situation, the interaction between the tip and the molecules will be responsible for the difference in friction forces. It could be expected that the main origin of this interaction was the shear between the tip and the casein layer. However, even though κ-casein layers have a much higher shear viscosity,[61] similar friction values are observed for both casein layers within this regime. This suggests that more components are needed to model the tip−sample interaction in this situation. Despite its possible applications for quantitative surface shear studies, this modeling is out of the scope of this work.

When the load is decreased from the previous situation, the same friction behavior is observed. This lasts until the total applied force reaches a similar value to that for which the protein aggregates started to be observed while increasing the load. Indeed, from the previous discussion, it is expected that the protein concentration will not reach the critical value for aggregate formation within the time scale for the acquisition of a friction−load curve. The force for which this regime, Reg5, ends is the one needed for a constant removal of the proteins in front of the tip. In fact, if the load is further decreased it is observed how the proteins rapidly diffuse in beneath the tip, which then slides against a compressed monolayer again.

These results show that FFS can be used to study both two-dimensional lateral diffusion of proteins on interfaces and, specifically, the diffusion of caseins on hydrophobic surfaces. This observation is highly relevant to understand how caseins work as stabilizers of suspensions/emulsions. For instance, it implies that if the casein coverage of a hydrophobic surface is locally damaged, molecules from the surrounding will diffuse back onto this area, recovering the coverage and avoiding the exposure of the inner hydrophobic substrate.

It also has been shown how the experimental procedure employed in friction measurements allows the study of wear. This is possible due to the 2D scanning of the sample and to the acquisition of its topography, which allow calculation of the wear volume during scans performed at different loads. However, some experimental aspects of friction measurements complicate the analysis of wear data. For instance, the scanning of the tip in opposite lateral directions implies that the molecules will also be pushed in both these directions. If the distance that they are pushed is lower than the scan lateral length, they will not contribute to the worn volume despite being displaced. The limited amount of material in protein monolayers can also influence wear data. For instance, the fact that the wear coefficient for β-casein monolayers is higher than the one for κ-casein monolayers is probably a consequence of the initial volume of the β-casein monolayers being higher.

(61) Murray, B. S.; Dickinson, E. *Food Sci. Technol. Int.* **1996**, *2*, 131–145.

5. Conclusions

Friction force spectroscopy measurements performed with nanometer-sized tips have been proved to be a powerful technique not only for the study of friction but also for the study of wear, cohesion, regeneration, and funicity of protein layers. The employment of nanometer-sized tips allows exerting and measuring a wide range of pressures, from the low values that allow studying the initial frictional behavior to the high values needed to remove these layers. Moreover, the employment of these tips allows imaging the topographic changes that follow the scratching of the layers. It was also shown that it is possible to study two-dimensional lateral diffusion of the proteins. Finally, the technique offers the possibility to perform wear studies on these surfaces.

The application of FFS to the study of β- and κ-casein layers has revealed important and interesting properties of these systems. Despite not being particularly lubricant surfaces, both the high pressures that they can withstand before complete removal and the fast regeneration of the layers after being damaged are properties that likely contribute to their efficiency as dispersing agents. The sensitivity of FFS has also been proven. Indeed, although differences in the friction coefficients were not resolved, differences in the cohesion between both types of layers, and the dependence of this parameter with pH and ionic strength, were clearly detected.

Acknowledgment. The foundation of Gustaf Th. Ohlsson, the Swedish Laryng Foundation, and Malmö University (Biofilms-research center for biointerfaces) are gratefully acknowledged for financial support. We also acknowledge Prof. Tommy Nylander for helpful discussions and for providing the reference β-casein sample.

Supporting Information Available: Caseins electrophoresis and calcium amount determination. Dependence of hydrophobic interaction with ionic strength. Representative lateral force profiles for the different friction regimes. Adsorption of β-casein at neutral pH. This material is available free of charge via the Internet at http://pubs.acs.org.